

Cross-Linking, Miscibility, and Interface Structure in Blends of Poly(2-ethylhexyl methacrylate) Copolymers. An Energy Transfer Study

Hung H. Pham,[†] J. P. S. Farinha,[‡] and Mitchell A. Winnik*

Department of Chemistry, University of Toronto, 80 St. George Street,
Toronto, Ontario, Canada M5S 3H6

Received November 1, 1999; Revised Manuscript Received May 16, 2000

ABSTRACT: We describe the miscibility of blends involving poly(ethylhexyl methacrylate) [PEHMA] latex copolymers using the direct nonradiative energy transfer (DET) technique. When the polymers in both components of a blend are PEHMA homopolymers, we obtain a fully mixed film. When one of the components in the blend is replaced with a PEHMA copolymer containing 5 mol % *tert*-butylcarbodiimidoethyl methacrylate (tBCEMA), we also obtain a fully mixed film. However, if a PEHMA copolymer containing 11 mol % methacrylic acid (MAA) is mixed with PEHMA homopolymer, the miscibility between the polymers is limited and is reduced further when the amount of MAA is increased to 20 mol %. Using a distribution model for energy transfer, we were able to determine the evolution of the interface thickness with annealing time. The maximum interface thickness attained in these blends decreases from $\delta = 15$ nm to $\delta = 8$ nm when the content of MAA in the blends increases from 11 mol % to 20 mol %. A freshly formed solvent-cast film prepared from a 1:1 blend of the PEHMA copolymer containing 11 mol % MAA and the PEHMA copolymer containing 5 mol % tBCEMA exhibits some polymer segregation. This persists in the solid film when the film is annealed for short times (20 min) at 60 °C. Over longer times, mixing of the copolymers occurs and reaches completion. We attribute this increase in miscibility to the formation of graft copolymer, which serves as a compatibilizing agent, through the reaction between the $-\text{COOH}$ and $-\text{N}=\text{C}=\text{N}-$ groups. When a film of the same composition is prepared from a blend of the two latex dispersions and annealed, a fully mixed film also results.

Introduction

In the preceding paper,¹ we described the use of direct nonradiative energy transfer (DET) experiments to determine the thickness of the interface in a blend of polymers of limited miscibility. We derived expressions that couple Helfand–Tagami² theory of the polymer segment density profile at the interface with the theory of energy transfer in restricted geometries.³ These equations were derived for the specific case of a blend composed of spherical droplets, all of the same size, dispersed in a continuous matrix of the second polymer. The equations were tested against a model system consisting of poly(butyl methacrylate) (PBMA) latex spheres labeled with phenanthrene as the donor dye, dispersed in anthracene-labeled poly(2-ethylhexyl methacrylate) (PEHMA) as the acceptor-labeled matrix.

In this paper, we extend these ideas to the case of a reactive blend in which the two components have limited miscibility in the as-prepared state but become miscible as the reaction proceeds. The blend consists of a mixture of two types of latex particles, both copolymers of PEHMA. One of the components is an EHMA copolymer containing 5 mol % of carbodiimide ($-\text{N}=\text{C}=\text{N}-$) groups, introduced during the emulsion polymerization via the *tert*-butylcarbodiimidoethyl methacrylate (tBCEMA). The second component is a copolymer of EHMA with methacrylic acid (MAA), containing either 11 or 20 mol % MAA groups. To study the amount

of mixing that occurs in these polymer blends, we follow the approach pioneered by Morawetz and co-workers⁴ and label the P(EHMA-*co*-MAA) component with a donor dye and its blend partner with an acceptor dye. The quantum yield of energy transfer (Φ_{ET}) provides a measure of the extent of miscibility of the two components.

PEHMA and the copolymers we examine all have glass transition temperatures (T_g) below room temperature. For many of the films we examine, the samples are prepared by mixing dispersions of the two types of latex particles, normally in a 1:1 particle ratio, and casting the aqueous solution onto a solid substrate. When a dispersion containing these latex particles is allowed to dry at room temperature, the particles become deformed during the drying process into cells with the shape of Voronoi polyhedra.⁵ In the initially formed latex film, the polymers are confined to separate cells. Upon standing at room temperature or upon annealing at elevated temperature, polymer diffusion can take place to increase the extent of mixing between the polymer molecules initially present in adjacent cells.

As in the preceding paper, we show that quantitative information about the breadth of the interface is available from analysis of the detailed shape of the donor fluorescence decay profile in blend films prepared from a mixture of two different labeled latex particles. The morphology of the system examined here is different in two respects from that described in the preceding paper. First, because both types of particles have similar glass transition temperatures, we believe that both are deformed into polyhedral cells. Nevertheless, at this stage of sophistication, we will treat the donor-labeled cell as though it were spherical. In addition, we examine blends prepared from a 1:1 mixture of the two types of latex particles. In the latex film, some of the neighboring cells

[†] Current address: Polymer Coating Technologies of Singapore Pte Ltd., 16 Joo Koon Crescent, Singapore 629018.

[‡] On leave from: Centro de Química-Física Molecular, complexo I, Instituto Superior Técnico, Av. Rovisco Pais, 1049–001 Lisboa, Portugal. E-mail: farinha@ist.utl.pt.

* To whom correspondence should be addressed. E-mail: mwinnik@chem.utoronto.ca.

will contain identical dyes. Polymer diffusion across this interface does not contribute to energy transfer. Only half of the surfaces in the blend separate donor- and acceptor-labeled polymer. Energy transfer across this interface determines the shape of the decay profile.

The reactive blend we consider is a classic example of a case in which reaction is coupled to diffusion. When the blend consists of a mixture of carbodiimide-containing latex and carboxylic acid-containing latex, the reactive groups in the newly formed film are confined to their separate cells. When these functional groups come into contact, they react to form an *N*-acylurea⁶ and in the process create a covalent bond between the two polymers. While some of these groups can react at the interface between the two types of cells, extensive reaction can only occur if the polymers containing the two types of reactive groups interdiffuse across the cell boundary. Polymer diffusion is necessary to bring the reactive groups together, but the chemical reaction introduces branches into the polymer, which retard the rate of diffusion, and creates cross-links that bring polymer diffusion to a halt. In this type of system, the growth in the quantum efficiency of energy transfer allows one to monitor the rate of polymer diffusion across the intercellular boundary⁷ and see how this rate is affected by the chemical reaction.

We are fortunate in this system that we can follow both the extent of polymer interdiffusion by DET measurements and the extent of chemical reaction by Fourier transform infrared spectroscopy (FTIR), taking advantage of the carbodiimide band at 2128 cm⁻¹.⁸ We are able to show that the two functional polymers have limited miscibility in the newly formed film. As they react, however, they become more miscible. We are able, by comparing DET and FTIR experiments, to show how the growth in polymer miscibility is coupled to the reaction between the carbodiimide groups and the carboxylic acid groups.

To establish a baseline to help us understand the processes that occur in the reactive blend, we also examine blends of the functional latex particles with PEHMA homopolymer latex particles. The analysis of this system takes us into a problem that has not been studied in any detail: the extent to which carboxylic acid groups present in a copolymer provoke phase separation when that copolymer is mixed with the corresponding homopolymers.⁹ One anticipates that the introduction of -COOH groups into a relatively nonpolar polymer like PEHMA could lead to phase segregation, depending on the -COOH content of the polymer. The extent of miscibility will depend on the magnitude of the Flory χ -parameter between the homopolymer and its carboxyl-containing copolymer.

In the experiments described below, we are able to show that the presence of 11 mol % MAA units in P(EHMA-co-MAA) copolymer is sufficient to induce phase separation when this polymer is blended with PEHMA. The blend of PEHMA with the copolymer containing 20 mol % MAA is even less miscible. The limited miscibility of these polymers would not be apparent by traditional methods. Both blends of PEHMA with P(EHMA-co-MAA) are transparent. In both blends, the glass transition temperatures (T_g) of the two components are too close for the presence of separate phases to be detected by differential scanning calorimetry or dynamic mechanical measurements.

Table 1. Recipe To Prepare PEHMA Seed Particles

	PEHMA seed particles		PEHMA seed particles
EHMA ^a (g)	40.0	NaHCO ₃ (g)	0.51
SDS ^b (g)	2.61	H ₂ O (g)	750
KPS ^c (g)	0.79		

^a (±)-2-Ethylhexyl methacrylate. ^b Sodium dodecyl sulfate. ^c Potassium persulfate.

When these blends are prepared from latex dispersions at temperatures close to the minimum film forming temperature, there is essentially no mixing in the freshly prepared film. When these films are heated, polymer diffusion takes place, leading to a limited extent of mixing of the two components. Blends of the same composition can also be prepared by dissolving the polymers in a common good solvent, such as tetrahydrofuran (THF). When this solution is cast onto a solid substrate and allowed to dry, phase separation occurs upon drying if the polymers are not fully miscible. For these samples, further demixing can occur when the films are annealed. DET experiments allow us to follow the time course of polymer mixing in the latex films¹⁰ and polymer demixing in the solvent-cast films. We obtain interesting insights into the nature of these polymer blends by comparing the results of experiments on latex films and solvent-cast films for each blend composition.

This paper is organized as follows: We begin with a brief Experimental Section, followed by a description of the characterization of the latex particles we examine. In this section we define our notation for the various labeled and functional latex polymers. We next address the issue of polymer miscibility by examining the quantum efficiency of energy transfer for latex blends (i.e., blends obtained by casting a film from a mixed dispersion of two types of latex particles) and comparing these results with those obtained for solvent-cast films of the same composition. We show how the reaction between the -N=C=N-containing latex and the -COOH-containing latex promotes miscibility of the initially phase-separated polymers. Finally, we examine the nature of the interface in the blends shown to have limited miscibility.

Experimental Section

Materials. (±)-2-Ethylhexyl methacrylate (EHMA, Aldrich) and methacrylic acid (MAA, Aldrich) were distilled prior to use. 1-Dodecylmercaptan (DM, Aldrich) and potassium persulfate (KPS, Aldrich) were used without further purification. 9-Phenanthrylmethyl methacrylate (PheMMA) and 9-anthrylmethyl methacrylate (AnMA) were prepared previously.¹¹ *tert*-Butylcarbodiimidoethyl methacrylate (tBCEMA) was synthesized as described previously.¹² Water was purified through a Milli-Q Water system.

Preparation of Seed and Labeled Particles. All labeled latex particles were prepared by a two-stage emulsion polymerization from a common seed under monomer-starved conditions.¹²

The seed particles were prepared by batch emulsion polymerization at 80 °C. A typical recipe and conditions to prepare the seed latex are shown in Table 1. These seed particles were then used to prepare various labeled latex particles.

Table 2 summarizes the recipes used in the second stage to prepare labeled latex without reactive functional groups, as well as those containing MAA (11 mol %) and tBCEMA (5 mol %). The labeled homopolymer latex samples, PEHMA-D or PEHMA-A, were prepared using the recipe listed in second column of the table. PheMMA was replaced by AnMA when

Table 2. Recipes Employed for the Second Stage in the Synthesis of the Various Latex Dispersions Examined^a

	PEHMA-D	D-MAA-11	A-tBCEMA-5
seed dispersion (g)	60.0	120.0	60.0
EHMA (g)	35.0	66.50	33.14
MAA (g)		3.50	
tBCEMA (g)			1.92
PheMMA (g)	0.49	0.77	
AnMA (g)			0.47
DM ^b (g)	0.32	0.61	0.32
KPS (g)	0.06	0.12	0.07
SDS (g)	0.70	1.29	0.70
NaHCO ₃ (g)			0.31
H ₂ O (g)	27.00	55.00	27.06
temp (°C)	80	80	60
feeding time (mL/min)	0.62	1.24	0.56

^a The second stage monomers were added to the reaction slowly, to maintain monomer-starved conditions. ^b 1-Dodecylmercaptan.

PEHMA-A was prepared. These latex dispersions were synthesized at 80 °C in the absence of additional NaHCO₃ in the second stage. The recipe listed in the third column was used to prepare a donor-labeled latex containing 11 mol % of MAA. We refer to this latex polymer as D-MAA-11, where D (donor) represents the type of the fluorescent dye, MAA (methacrylic acid) represents the type of the reactive group, and the number 11 is the amount (in mol %) of the MAA used in the original recipe. The other carboxylic acid-containing latex, D-MAA-20, was prepared in a similar manner, but with 20 mol % of MAA. These MAA-containing particles were prepared at 80 °C in the absence of additional NaHCO₃. Note that the amount of seed particles and ingredients used to prepare the two MAA-containing latex are doubled. The recipe shown in the last column was used to prepare two dispersions of acceptor-labeled latex particles containing 5 and 11 mol % of tBCEMA. We refer to these latex copolymers as A-tBCEMA-5 and A-tBCEMA-11, respectively, where A (acceptor) represents the type of the fluorescent dye and tBCEMA (*tert*-butylcarbodiimidoethyl methacrylate) represents the type of the reactive group. The numbers 5 and 11 refer to the amount (in mol %) of the tBCEMA used in the original recipe. These tBCEMA-containing particles were prepared at 60 °C in the presence of additional NaHCO₃ in the feed stage. In all of the recipes, the amount of chain transfer reagent and the fluorescent dye were kept at 1 wt % and 1 mol %, respectively.

Particle sizes and particle size distributions were determined by dynamic light scattering at 22 °C at an angle of 90°, employing a Brookhaven BI-90 particle sizer. Gel permeation chromatography (GPC) was carried out on an apparatus equipped with a Waters pump, two Ultrastaygel columns (HR 3 and 4), a fluorescence detector, and a refractive index detector. For the fluorescence detector, the excitation wavelength was set at 300 nm for Phe and 350 nm for An. Reagent grade THF was used as the solvent with a flow rate of 0.4 mL/min at 30 °C. Linear poly(methyl methacrylate) standards were used to calibrate the columns.

Preparation of Urea-Containing Particles. An aliquot (10 mL) of the A-tBCEMA-5 dispersion was treated with a stoichiometric amount of propanoic acid at room temperature. The fraction of -N=C=N- groups remaining at various times was monitored by FTIR. At the end of 60 h the reaction was complete, and we assume that all of the *tert*-butylcarbodiimide groups were converted to *tert*-butylurea groups. We refer to this modified polymer as A-tBUEMA, where U refers to urea.

Preparation of Dispersion- and Solvent-Cast Films. Films were prepared on quartz plates for energy transfer (ET) measurements and on CaF₂ disks for FTIR measurements. These films were often prepared from the same mixture of labeled latex particles.

A 1:1 mixture of Phe- and An-labeled latex particles was first prepared by mixing the two dispersions (at about 30 wt % solids) and then dividing the sample into two portions. To prepare a mixture of latex containing the carbodiimide-

containing particles, the carboxylic acid-containing particles and the PEHMA-D latex were first neutralized with aqueous ammonia to pH 8. One portion of the mixture was cast directly onto quartz plates and onto CaF₂ disks. The CaF₂ disks and quartz plates were then placed under an inverted Petri dish at either 22 or 4 °C. The drying time ranged from 5 to 7 h for the films dried at 22 °C and 1 to 2 days for the films dried at 4 °C. All films were transparent and crack-free. The typical thickness of films for ET measurements was about 0.3 mm and for FTIR measurements about 1–2 μm. We began the first ET and FTIR measurements about 1 h after the last wet spot of the film disappeared. When we consider the time evolution of the film, we arbitrarily take this time to be *t*₀.

The other portion of the mixture was freeze-dried for 1 h. Then a small portion of the freeze-dried sample was dissolved in THF and cast onto a CaF₂ disk for FTIR measurements and onto a quartz plate for ET measurements. The drying time for these solvent-cast films ranged from 5 to 15 min. Typical thickness of these films was 1 μm. Another small portion of the freeze-dried polymers was mixed with dry KBr powder and then pressed into a thin KBr disk for an FTIR measurement. The FTIR spectrum of this KBr-disk sample was used to determine the amount of -N=C=N- groups lost during the drying process to prepare the dispersion-cast and THF-cast films. The survival of carbodiimide groups in these latex films is described in detail elsewhere.^{12,13}

FTIR Measurements. All FTIR measurements, with a resolution of 4.0 cm⁻¹, were made with a Perkin-Elmer FTIR spectrometer Spectrum 1000. Before the first measurement in a series, the CaF₂ disks containing the polymer films were mounted on FTIR holders. After the measurement was complete, the entire FTIR holders were then placed directly on an aluminum plate under a Petri dish in a forced-air oven at 60 °C for different amounts of time. The FTIR holders were periodically removed, cooled to room temperature, and remeasured.

The -N=C=N- functionality has a characteristic band at 2128 cm⁻¹ in the FTIR spectrum. We rely on the intensity ratio of this band to that of the band at 1380 cm⁻¹, (*I*_{N=C=N}/*I*₁₃₈₀), to determine the amount of -N=C=N- groups lost during the THF and water evaporation. The band at 1380 cm⁻¹ corresponds to a C-H bending vibration of the polymer.^{14,15} We also rely on this intensity ratio, measured as a function of time, to follow the cross-linking reaction between the -COOH and -N=C=N- groups.

To determine the amount of -N=C=N- groups lost during THF or water evaporation, we compared the (*I*_{N=C=N}/*I*₁₃₈₀) ratio in the FTIR spectrum of the KBr-pressed sample to that of either the dispersion- or THF-cast sample measured at *t*₀. To follow the reaction between the -N=C=N- groups and the -COOH groups, we employ eq II.1

$$-\text{N}=\text{C}=\text{N}- \text{ reacted } (\%) = \left(1 - \frac{(I_{\text{N}=\text{C}=\text{N}}/I_{1380})_t}{(I_{\text{N}=\text{C}=\text{N}}/I_{1380})_{t_0}} \right) \times 100 \quad (\text{II.1})$$

where (*I*_{N=C=N}/*I*₁₃₈₀)_{*t*₀} and (*I*_{N=C=N}/*I*₁₃₈₀)_{*t*} are the ratios of the -N=C=N- absorbance intensity to the absorbance intensity at 1380 cm⁻¹ of a newly formed film (*t*₀) and of the same film annealed at a particular time *t*.

Fluorescence Decay Measurements. All fluorescence decay measurements employed the time-correlated single photon counting technique,¹⁶ using a pulsed deuterium lamp as the excitation source. In the Phe-An system employed here, we set the excitation wavelength at 300 nm and the emission wavelength at 350 nm. An interference filter for emission was chosen at 350 ± 5 nm. In a series of fluorescent decay measurements, the quartz plates containing polymer films were placed in quartz tubes and flushed with N₂ gas before they were measured. After each measurement, the quartz plates were removed from the quartz tubes and placed directly on an aluminum plate under a Petri dish in a forced-air oven at 60 °C for different amounts of time. The quartz plates were

Table 3. Notation Used To Identify the Various Polymer Blends Examined

type of latex polymer	abbreviated name
P(EHMA- <i>co</i> -PheMMA)	PEHMA-D
P(EHMA- <i>co</i> -AnMA)	PEHMA-A
P(EHMA- <i>co</i> -MAA- <i>co</i> -PheMMA)	D-MAA-11
	D-MAA-20
P(EHMA- <i>co</i> -tBCEMA- <i>co</i> -AnMA)	A-tBCEMA-5
	A-tBCEMA-11

periodically removed, cooled to room temperature, and remeasured under a N₂ atmosphere in quartz tubes.

Fluorescence Decay Analysis. The quantum efficient of energy transfer, Φ_{ET} , is defined as¹⁷

$$\Phi_{ET} = 1 - \frac{\int_t I_D(t) dt}{\int_t I_D^0(t) dt} \quad (\text{II.2})$$

where $I_D(t)$ and $I_D^0(t)$ represent the decay functions of donor fluorescence in the presence and absence of acceptor, respectively. In the presence of acceptor the decay of the donor is faster due to energy transfer and the corresponding integrated intensity is smaller, increasing the value of Φ_{ET} . The integrals in eq II.2 correspond to the areas under the donor decay curves, normalized at time zero. The $I_D^0(t)$ decay profile of the sample containing only donor is exponential; the integral in the denominator of eq. II.2 is equal to the donor lifetime τ_D . To obtain the area under the fluorescence decay of the donor in the presence of acceptor, we fitted each decay curve to the empirical equation (eq 1) given in the preceding paper¹ and used the fitting parameters to calculate analytically the integral of $I_D(t)$ from $t = 0$ to $t = \infty$. Φ_{ET} values were then calculated with eq II.2.

To obtain information about the interface thickness from the experimental fluorescence decay profiles, the experimental fluorescence decay profiles $I_D^{exp}(t)$ obtained for films of 1:1 blends of anthracene-labeled PEHMA and phenanthrene-labeled PEHMA-MAA latex particles were compared with simulated fluorescence decay profiles $I_D^{conv}(t)$ obtained as described in the preceding paper.¹

Results and Discussion

Characterization of Labeled Latex Polymers. All latex particles were synthesized by seeded emulsion polymerization, with the fluorescent and functional comonomers being introduced only in the second stage under monomer-starved conditions.^{10,11} The seed particles, prepared by batch emulsion polymerization, consist of PEHMA homopolymer. The PEHMA seed particles have a mean diameter of about 50 nm and a high molecular weight (PEHMA: $M_w = 700\,000$, $M_w/M_n = 2.65$). From these seed particles, we prepared six batches of labeled latex, two of which contain no reactive comonomers. The polymer compositions of the individual latex samples are listed in Table 3, along with an abbreviated name. In the abbreviated name, the base polymer is sometimes not included, but it implies the PEHMA polymer.

The characteristics of these labeled latex particles are summarized in Table 3. Since they were prepared from similar recipes, the different latex particles have similar particle sizes and size distributions, solids content, molecular weights, and molecular weight distributions. GPC analysis with tandem fluorescence and refractive index detectors showed that fluorescent dye molecules are randomly distributed in the polymer and that there were no small molar mass fluorescent molecules in the samples. The synthesis of the methacrylic acid copoly-

mer latex was designed to avoid the concentration of carboxylic acid groups at the surface of the particles. Feng and Winnik^{7,11} studied a similar system involving a latex copolymer of butyl methacrylate and methacrylic acid prepared via emulsion polymerization under monomer-starved conditions. These authors showed that the acid groups were distributed in an essentially uniform way throughout the latex particle and not segregated to the particle surface. Since the P(EHMA-*co*-MAA) particles employed here were prepared by an almost identical procedure in which EHMA was substituted for BMA, we expect a similar distribution of acid groups. The carbodiimide content in the carbodiimide-containing latex was determined by Fourier transform infrared spectroscopy (FTIR) for samples dissolved in CHCl₃. We found that almost all (98%) of the $-N=C=N-$ groups were incorporated into the latex polymer. The conditions to optimize the survival of the $-N=C=N-$ functionality, both during the emulsion polymerization and during storage of these carbodiimide-containing latex dispersions, have been reported elsewhere.^{12,13}

Energy Transfer Efficiency Experiments. We employ Φ_{ET} to characterize the miscibility of PEHMA copolymers. In the latex system examined here, we label one type of latex with Phe and the other type of latex with An. When these labeled particles are mixed in dispersion, deposited on a substrate, and water is allowed to evaporate, a continuous film is formed. In the newly formed film, before any interparticle diffusion has occurred, the Phe- and An-labeled polymers should still be confined within their own cells. Φ_{ET} is small because only cross-boundary energy transfer can occur. For a low- T_g polymer like PEHMA ($T_g = -10\text{ }^\circ\text{C}$),¹⁸ determining this initial quantum yield poses an experimental challenge, because films formed at room temperature provide the system with time for some local polymer diffusion to occur while the film is drying. Our strategy for minimizing the extent of polymer diffusion during film formation was to prepare films in a cold room at 4 $^\circ\text{C}$. These films, which took about 2 days to dry, were kept cold (on ice) while the film was transferred to the room where the decay profile was to be measured. The sample holder was cooled to ca. 4 $^\circ\text{C}$ during the measurement. In this way, we obtained initial Φ_{ET} values on the order of 0.05. The extent of DET increased afterward, as the sample was permitted to warm to room temperature (22 $^\circ\text{C}$). Films formed at room temperature have initial Φ_{ET} values closer to 0.12.

If the sample is then allowed to stand at room temperature or heated to increase the polymer diffusion rate, polymers will diffuse from one cell to the adjacent cells, bringing the Phe and An groups into proximity. Φ_{ET} increases and evolves to its maximum value. If the polymers in adjacent cells are fully miscible, this maximum value should correspond to that obtained from films prepared from a THF solution of the same polymer blend. In the THF solution, the Phe- and An-labeled polymers are homogeneously mixed because THF is a good solvent for the PEHMA copolymers. For homopolymers that differ only in their fluorescent label, the two types of polymers are miscible in the bulk state. The homogeneous mixture in the solution will carry forward into the films when the solvent is evaporated. For other pairs of miscible polymers the same maximum Φ_{ET} value should be obtained by solvent-cast a film, and the magnitude of Φ_{ET} should not change when the film is annealed.

Table 4. Characteristics of the Labeled Latex Polymers

	particle diameter (nm)	solids content (%)	M_w , M_w/M_n	pH	carbodiimide content (%)
PEHMA-D	98	30.9	39 000, 2.44	5	
PEHMA-A	97	31.1	56 000, 2.07	5	
D-MAA-11	101	31.2	41 000, 1.95	5	
D-MAA-20	113	31.0	50 500, 2.35	5	
A-tBCEMA-5	106	31.9	63 000, 3.15	8	98
A-tBCEMA-11	102	31.7	45 500, 2.39	8	98

Immiscible polymer pairs should behave differently. In films prepared from latex blends, one expects Φ_{ET} to increase, accompanying some segment mixing across the interface between adjacent cells. The limiting value of Φ_{ET} should be significantly less than that for the fully mixed film. For films prepared by solvent casting, some polymer demixing will occur as the solvent evaporates. Some further segregation may occur as the solid film is annealed. In this case, Φ_{ET} will decrease from the initial value.

PEHMA-D/PEHMA-A Blend. We first examine the miscibility of PEHMA-D + PEHMA-A latex polymers. Here, aside from the label, the polymers are chemically identical. One would expect that a fully mixed film should result. We prepared two films from a 1:1 mixture of these labeled latex polymers. One film was cast directly from the latex dispersion. The other was prepared first freeze-drying an aliquot of the mixed dispersion. This mixture was then dissolved and cast onto the substrates. In the newly formed THF-cast film, we obtain $\Phi_{ET} = 0.52$. When the same film is annealed at 60 °C for various amounts of time, Φ_{ET} remains at 0.52 ± 0.01 . This result indicates that when the Phe- and An-labeled polymers are fully mixed in the freshly prepared film and that no changes occur when the film is annealed for various times at 60 °C. For films prepared at 4 °C from the latex dispersions, we obtain $\Phi_{ET} = 0.06$. We believe that little polymer diffusion occurs at this temperature and that cross-boundary DET is the major contribution to this value. When the same film is annealed at 60 °C, Φ_{ET} increases to 0.38 in 2 min and then to 0.49 in 12 min. This result indicates that diffusion leading to polymer mixing has occurred. The value of Φ_{ET} at 0.49 signifies that the mixing between PEHMA-D and PEHMA-A polymers is nearly complete and will reach completion if the film is annealed for a long time. The Φ_{ET} values obtained from the dispersion-cast and THF-cast films at different times are plotted in Figure 1. We accept $\Phi_{ET} = 0.52$ for fully mixed films and use it as a reference value.

A-tBCEMA-5/PEHMA-D Blend. We repeated these experiments on films prepared from the blend of PEHMA-D plus A-tBCEMA-5. We plot Φ_{ET} as a function of annealing time in Figure 2 for both a solvent-cast film and a latex film. Here we see that Φ_{ET} behaves in a similar way as the blend of PEHMA-D and PEHMA-A shown in Figure 1: For the THF-cast films $\Phi_{ET} = 0.52$ and remains constant as the film is annealed. For the latex film, the initial value of Φ_{ET} is low, reflecting the compartmentalization of the Phe and An groups, but Φ_{ET} evolves upon annealing to a value of 0.52. This result indicates that polymers in the A-tBCEMA-5/PEHMA-D blend are miscible.

D-MAA/PEHMA-A Blend. In contrast to the results described above, blends of PEHMA with MAA-containing copolymers exhibit the behavior expected for a blend of polymers with limited miscibility. The first example of this type of blend we consider consists of equal amounts of D-MAA-11 and PEHMA-A latex polymers.

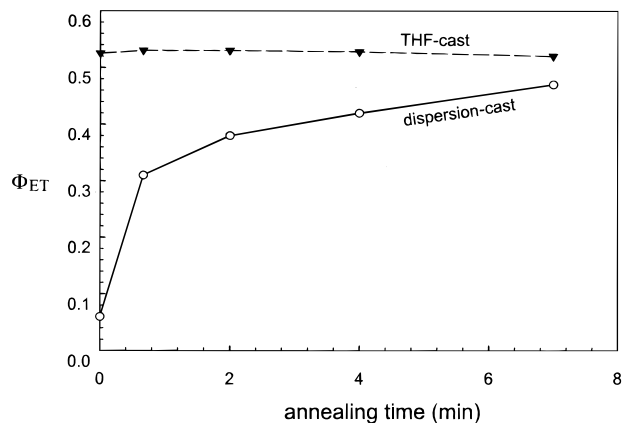


Figure 1. Plots of Φ_{ET} vs time for a latex film and a THF-cast film prepared from the PEHMA-D/PEHMA-A blend and annealed at 60 °C. The latex film was prepared at 4 °C while the THF-cast film was dried at 22 °C.

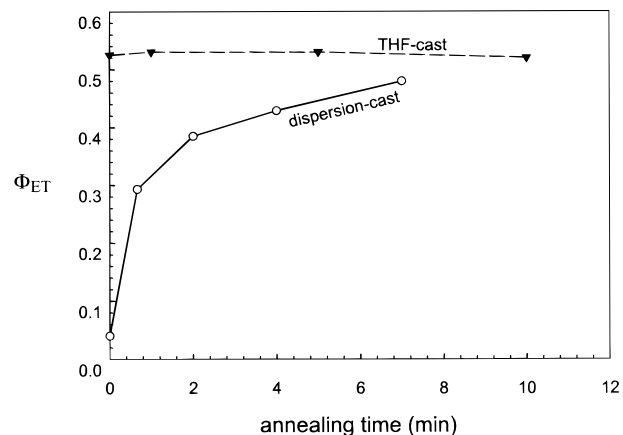


Figure 2. Plots of Φ_{ET} vs time for a latex film and a THF-cast film prepared from the A-tBCEMA-5/PEHMA-A blend and annealed at 60 °C. The latex film was prepared at 4 °C while the THF-cast film was dried at 22 °C.

We prepared latex films from a blend of the two dispersions and a solvent-cast film from a solution of the two polymers in THF. In Figure 3 we show the results obtained for films annealed at 60 °C. In the latex film formed at 4 °C, $\Phi_{ET} = 0.03$. When this film is annealed, the Φ_{ET} values increase to 0.21 in 10 min and then slowly increase to 0.24 over 1 h. The increase in Φ_{ET} signifies that polymer mixing occurs. The limiting value is significantly less than 0.52, the value expected for complete mixing. We take this result to indicate that the two polymers have only limited miscibility.

Further evidence to support the limited miscibility of these latex polymers is obtained from the solvent-cast film. When a freshly formed film prepared from a THF solution of the same blend is examined, we obtain $\Phi_{ET} = 0.40$, i.e., less than full mixing. This result indicates that the D-MAA-11 copolymer and PEHMA-A homopolymer segregate during THF evaporation. When this film is then annealed at 60 °C, Φ_{ET} decreases to

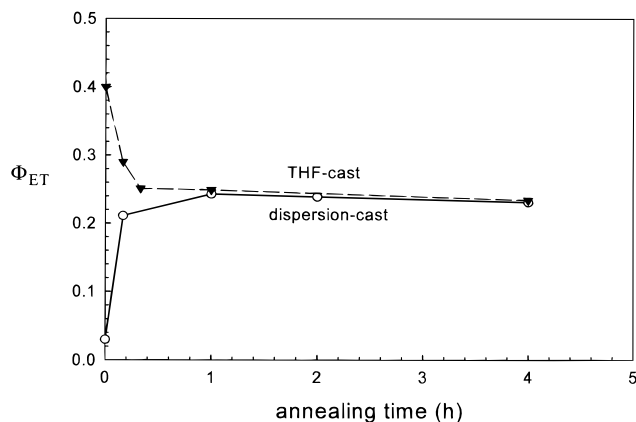


Figure 3. Plots of Φ_{ET} vs time for a latex film and a THF-cast film prepared from the D-MAA-11/PEHMA-A blend and annealed at 60 °C. The latex film was prepared at 4 °C, and the THF-cast film was dried at 22 °C.

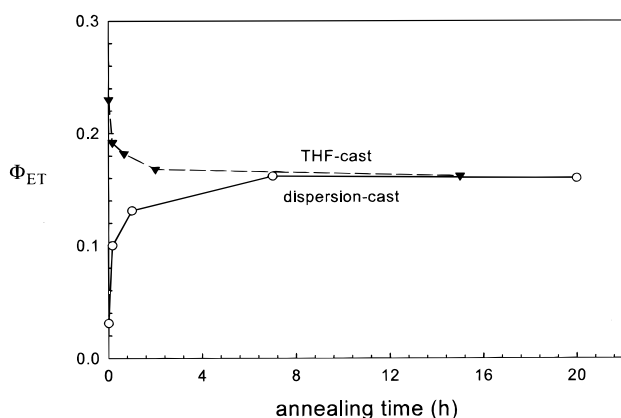


Figure 4. Plots of Φ_{ET} vs time for a latex film and a THF-cast film prepared from the D-MAA-20/PEHMA-A blend and annealed at 60 °C. The latex film was prepared at 4 °C, and the THF-cast film was dried at 22 °C.

0.25 over 20 min, indicating that further demixing takes place, leading to increased separation of the Phe- and An-labeled polymers. At longer annealing time (e.g., 4 h), Φ_{ET} decreases to 0.23, a value similar to that obtained from the annealed latex film.

The second example is a blend with an increased amount of MAA in the copolymer, 20 mol %. In Figure 4 we plot Φ_{ET} values vs annealing time for films prepared from the D-MAA-20/PEHMA-A blend. In the freshly formed film prepared at 4 °C from the latex dispersion, $\Phi_{ET} = 0.03$. When this film is annealed, Φ_{ET} increases to 0.14 over 1 h and then to a maximum value of 0.16 over 7 h. This value is even lower than that obtained from the D-MAA-11/PEHMA-A blend (0.24), which indicates that when the MAA content of the copolymer is doubled, the miscibility between D-MAA-20 and PEHMA-A polymers is further reduced. With longer annealing time, 20 h, a small decrease in Φ_{ET} is observed (Figure 4). When a film of D-MAA-20/PEHMA-A blend is freshly prepared from THF solution, we obtain $\Phi_{ET} = 0.23$, smaller than that (0.40) obtained for the solvent-cast film prepared from D-MAA-11 + PEHMA-A. Here we infer that the polymers segregate substantially as the solvent evaporates. When this film is annealed, Φ_{ET} decreases and approaches 0.16 over 15 h, a value close to that obtained from the annealed latex film.

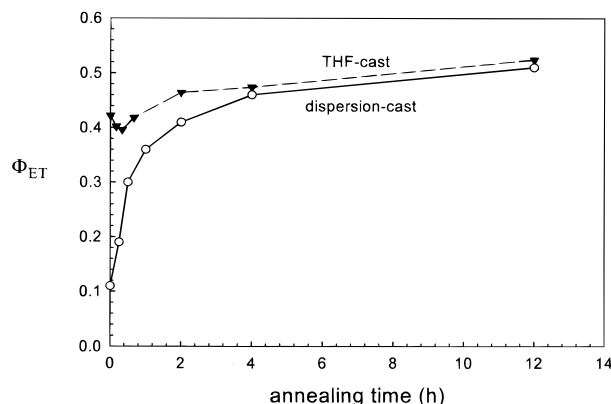


Figure 5. Plots of Φ_{ET} vs time for a latex film and a THF-cast film prepared from the D-MAA-11/A-tBCEMA-5 blend and annealed at 60 °C. Both latex film and the THF-cast film were dried at 22 °C.

Reactive Blends. The blend of D-MAA-11 + A-tBCEMA-5 constitutes a reactive blend in which the two polymers contain functional groups that can react to produce a graft copolymer initially and eventually a cross-linked network. The reaction is that of the carbodiimide group of A-tBCEMA-5 with the carboxylic acid group of D-MAA-11 to form an *N*-acylurea. When we prepared blends of the two latex dispersions, we were careful to neutralize the D-MAA-11 dispersion to pH 8 with ammonia before combining it with the $-N=C=N-$ -containing latex. In this way, we could minimize the rate of carbodiimide hydrolysis in the mixed dispersion. When we examine a film freshly prepared at room temperature from this latex blend, $\Phi_{ET} = 0.11$. It is likely that both cross-boundary DET and local interdiffusion contribute to this value, since this film is formed at 22 °C, not 4 °C. When the film is annealed at 60 °C, Φ_{ET} increases to 0.36 over 1 h and then to 0.52 in 12 h. The data are plotted in Figure 5. This is, for us, a very satisfying result, because it indicates that a fully mixed film is obtained. We note, however, that it takes hours for the polymers of this blend to mix completely whereas for the polymers of the PEHMA-D/PEHMA-A blend, full mixing occurs on the time scale of minutes.

It is known that the rate of polymer diffusion varies with chain length and is sensitive to the presence of branching.¹⁹ For linear polymers shorter than the entanglement molecular weight, the diffusion coefficient D_i characterizing the diffusion of a given chain of length N_i decreases as N_i^{-1} . For linear polymers longer than the entanglement molecular weight, the diffusion coefficient D_i decreases as N_i^{-2} . In the D-MAA-11 + A-tBCEMA-5 blend examined here, polymer diffusion and the cross-linking reaction are coupled. The polymer chain length and the extent of branching increase as the reaction proceeds. It, therefore, takes longer time for the polymers to mix.

For comparison, we examine the Φ_{ET} vs time curve obtained for the blend of these polymers from a THF-cast film. This curve is plotted as the triangles in Figure 5. This curve shows several interesting aspects. In the newly formed film, $\Phi_{ET} = 0.42$, a value lower than 0.52. This result indicates that segregation of D-MAA-11 and A-tBCEMA-5 polymers occurs as the THF evaporates. When this film is annealed at 60 °C, Φ_{ET} decreases to 0.40 over the first 20 min. Demixing of the polymers contributes to a decrease in Φ_{ET} . Upon longer annealing, Φ_{ET} begins to increase. To rationalize this result, we

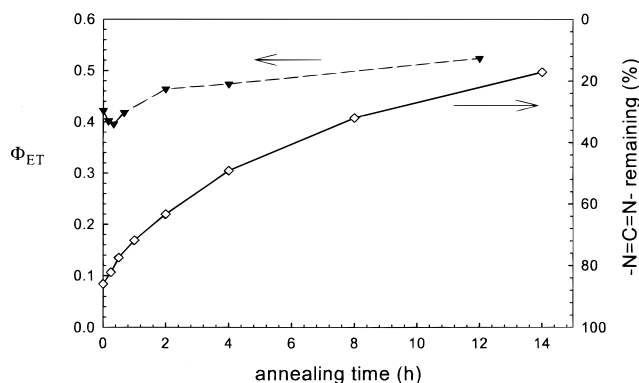


Figure 6. Plots of Φ_{ET} and percentage of $-N=C=N-$ remaining vs time for THF-cast films prepared from the D-MAA-11/A-tBCEMA-5 blend and annealed at 60 °C. The films were formed at 22 °C.

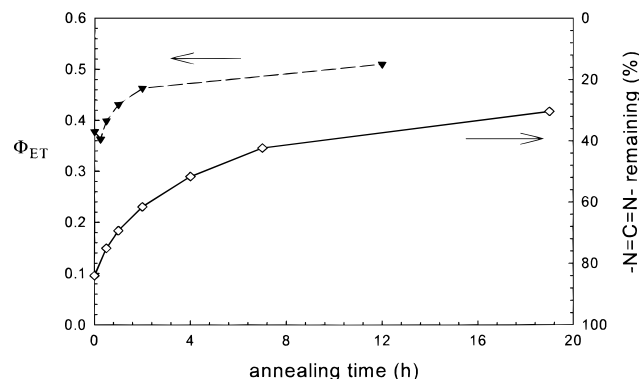


Figure 7. Plots of Φ_{ET} and percentage of $-N=C=N-$ remaining vs time for THF-cast films prepared from the D-MAA-20/A-tBCEMA-11 blend and annealed at 60 °C. The films were formed at 22 °C.

imagine that the reaction between the $-N=C=N-$ groups and the $-COOH$ groups promotes miscibility. At long times, Φ_{ET} reaches 0.52, indicating that the polymers in the film are fully mixed, at least on the scale of the energy transfer distance R_0 .

We can compare the state of mixing as indicated by Φ_{ET} with the extent of carbodiimide reaction, monitored by the decrease in the FTIR intensity at 2128 cm^{-1} . The results for the THF-cast film are plotted in Figure 6, along with the corresponding Φ_{ET} value for comparison. During film preparation (THF evaporation), we detect that 14% of the $-N=C=N-$ groups are lost. When the same film is annealed for 0.5 h, the loss of $-N=C=N-$ groups increases to 22%. Over this time, polymer demixing occurs. When the same film is annealed for 15 h, the conversion of the $-N=C=N-$ groups increases to 83%. During this time, polymer mixing begins to dominate and is complete in 12 h at 60 °C.

Next we consider what happens to the polymer miscibility when we double the amount of the reactive groups in the two components of the reactive blend, from 11 to 20 mol % for MAA and from 5 to 11 mol % for tBCEMA. In Figure 7, we plot Φ_{ET} values vs time for data obtained from the THF-cast films. On the right-hand axis of the plot, we also indicate the extent of the reaction of the $-N=C=N-$ groups. Both films were prepared from the same THF solution of D-MAA-20 plus A-tBCEMA-11. In the newly formed film, we obtain $\Phi_{ET} = 0.38$, a value lower than that of the blend containing the lower amount of the reactants ($\Phi_{ET} = 0.42$). This result indicates that as the concentration of the reactive

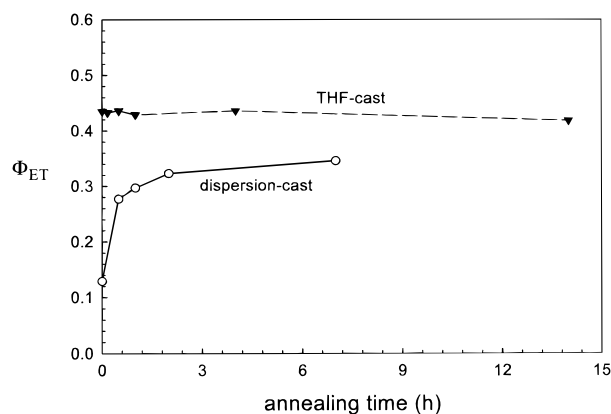


Figure 8. Plots of Φ_{ET} vs time for a latex film and a THF-cast film prepared from the D-MAA-11/A-tBUEMA blend and annealed at 60 °C.

groups increases, the degree of polymer segregation in the solvent-cast film increases, even though 16% of the $-N=C=N-$ groups react during the drying process. When these films are annealed for short periods of time (25 min) at 60 °C, polymer demixing occurs as shown by a decrease in Φ_{ET} from 0.38 to 0.36. Over this time, the extent of the carbodiimide reaction increases to 25%. When the same film is annealed for longer times, Φ_{ET} increases to 0.43 over 1 h and then reaches its limiting value of 0.51 over 12 h. This result indicates that upon prolonged annealing the polymers in the film become completely mixed. During this time, the extent of the carbodiimide reaction increases to about 60%. The increase in the reactant density in the two polymers does not prevent complete mixing of the polymer molecules in the system.

A Model System, the D-MAA-5/A-tBUEMA-5 Blend. In the reactive blend, all of the carbodiimide groups and half of the carboxylic acid groups react to form an *N*-acylurea. Under these circumstances, the two different polymers appear to be fully miscible at the molecular level. We were curious to know whether miscibility was driven by graft copolymer formation or whether the P(EHMA-*co*-MAA) polymer is intrinsically miscible with a PEHMA copolymer containing urea groups. Dialkyl ureas are both hydrogen bond donors through their N-H bonds and hydrogen bond acceptors. To investigate this issue, we prepared a latex containing *tert*-butylureidoethyl groups by acid-catalyzed hydrolysis of the $-N=C=N-$ groups of the A-tBCEMA-5 dispersion. These particles have the same particle size and the same polymer molecular weight and molecular weight distribution as the carbodiimide-containing latex particles. We refer to this modified polymer as A-tBUEMA, where U refers to urea.

In Figure 8 we examine the behavior of a 1:1 blend of D-MAA-11 plus A-tBUEMA and compare a film cast from a solution in THF with that of a latex film. In the newly formed film prepared from the latex dispersion at 22 °C, we obtain $\Phi_{ET} = 0.13$. Upon annealing at 60 °C, Φ_{ET} increases rapidly to 0.28 over 0.5 h and then to 0.35 over 7 h. In the newly formed film cast from THF solution, we obtain $\Phi_{ET} = 0.44$, a value indicating that some segregation of the polymers occurs during evaporation of the solvent. When the same film is annealed at 60 °C for 14 h, Φ_{ET} remains essentially unchanged. These results suggest that the interaction between the $-COOH$ groups on one copolymer and the dialkyl urea groups on the second copolymer enhances the polymer

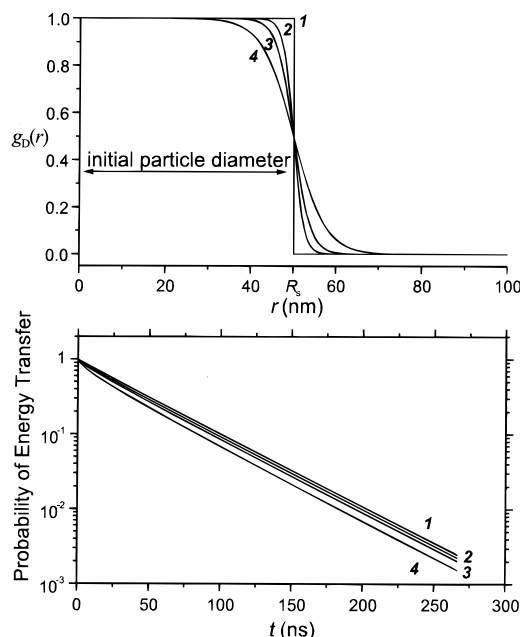


Figure 9. Radial distribution (top) of a donor labeled polymer particle of radius $R_s = 50$ nm and various interface thicknesses: $\delta = 0$ nm (1), $\delta = 5$ nm (2), $\delta = 8$ nm (3), and $\delta = 15$ nm (4). The corresponding donor decay functions (eqs II.3 and II.4) for 1:1 blends of acceptor-labeled PEHMA and donor-labeled PEHMA-MAA are also shown (bottom).

miscibility compared to that of P(EHMA-co-MAA) + PEHMA. However, the formation of graft copolymers also contributes to reaching full miscibility when the D-MAA-11 plus A-tBCEMA-5 blend is annealed (Figure 5).

Interface Thickness in PEHMA/PEHMA-MAA Blends. In this section we return to the blends of PEHMA homopolymer latex with the PEHMA copolymers containing 11 and 20 mol % methacrylic acid (MAA). In the previous discussion, we described the extent of miscibility of these polymers in terms of the ET quantum efficiency Φ_{ET} . These values, calculated via eq II.1, were obtained in a model-free way with minimal assumptions in the data analysis. We would like to explore the possibility that deeper information about the blends can be obtained, in terms of a model, from the detailed shape of the donor fluorescence decay profile $I_D(t)$. We employ the model developed in the previous paper¹ that combines the Helfand–Tagami (HT) description of the polymer segment density distribution across the interface in a polymer blend² with the theory of energy transfer in restricted geometries.³ We assume that the donor groups in the system have the same distribution as the segments of the polymer to which they are attached and that the distribution of acceptors follows the segment distribution of the acceptor-labeled polymer. In Figure 9 (top) we plot the donor distribution functions for a blend consisting of particles of radius $R_s = 50$ nm in a matrix of a second polymer, for four different interface thicknesses: $\delta = 0$ nm, $\delta = 5$ nm, $\delta = 8$ nm, and $\delta = 15$ nm.

The experiments described in this paper differ in a small but important way from those described in the preceding paper. In those experiments, we used a 14:1 particle ratio to ensure that each donor-labeled cell in the latex film was surrounded by an acceptor-labeled matrix. Here, because of our interest in the cross-linking reaction, we employ a 1:1 mixture of the two types of

latex particles. In the film, on average, only half of the surface of a cell containing donor-labeled polymer is in contact with acceptor-labeled polymer. To proceed with the analysis of the interface, some additional assumptions are necessary. We begin by assuming that for this system the fluorescence decay rate depends on the donor and acceptor distributions across the interface in the same way as described in the preceding paper. There we showed (eqs 11a and 11b) that for energy transfer in spherical systems²⁰ the donor decay function for a delta-pulse excitation is given by the expressions

$$F_D(t) = \exp\left(-\frac{t}{\tau_D}\right) \int_{V_s} C_D(r_D) \varphi(t, r_D) r_D^2 dr_D \quad (\text{II.3})$$

$$\varphi(t, r_D) = \exp\left(-\frac{2\pi}{r_D} \int_{R_e}^{\infty} \{1 - \exp[-w(r)t]\} \left[\int_{|r_D-r|}^{r_D+r} C_A(r_A) r_A dr_A \right] r dr\right) \quad (\text{II.4})$$

where V_s is the volume containing the donors, τ_D is the unquenched fluorescence lifetime of the excited donor, and $\varphi(t, r_D)$ is the probability of energy transfer of a donor located at r_D . $C_D(r)$ and $C_A(r)$ are the respective concentration profiles of the donor and acceptor across the interface between donor- and acceptor-labeled cells in the film. We take one donor-labeled particle as representative and use it as a reference. We consider that half of the interface of this donor-labeled reference particle is in contact with other donor-labeled polymer. For this part of the reference particle surface $\varphi(t, r_D) = 1$ and $C_D(r) = 1$. The other half of the donor-labeled reference particle surface is surrounded by acceptor-labeled polymer.

As described in the preceding paper, it is not possible to extract the shape or width of the interface directly from the shape of the donor fluorescence decay profile. Instead, one simulates a series of fluorescence decay curves using input parameters appropriate for the experiment, but for various assumed values for the interface thickness δ . To calculate each simulated fluorescence decay curve, we assume a value of δ , calculate $C_A(r_A)$ and $C_D(r_D)$ with eqs 1 and 2 of the preceding paper,¹ and then use eqs II.3 and II.4 to calculate $\varphi(t, r_D)$ and $F_D(t)$. The donor survival probability $F_D(t)$ is convoluted with the instrument response function $L(t)$ of each experiment, and Poisson noise is added to the resultant curve to obtain the simulated fluorescence decay profile $F_D^{\text{conv}}(t)$. The fitting process (eq 13, preceding paper) compares the experimental decay curve $F_D^{\text{exp}}(t)$ with $F_D^{\text{conv}}(t)$, taking account of a small light scattering contribution to the experimental data.

In Figure 9 (bottom) we plot several donor decay function curves calculated for parameters corresponding to blends of PEHMA and PEHMA-MAA. We show the simulated decays and the corresponding donor distribution functions for interface thicknesses $\delta = 0$ nm, $\delta = 5$ nm, $\delta = 8$ nm, and $\delta = 15$ nm. In the simulations we used $\kappa^2 = 0.478$, $R_0 = 2.3$ nm, a cutoff distance $R_e = 0.5$ nm, and $\tau_D = 45.5$ ns. This value of τ_D corresponds to that measured for a film cast from a PEHMA-MAA polymer labeled with donor. For the simulations, the particle radius was $R_s = 50$ nm, the ratio of acceptor to donor labeled particles was 1:1, and the acceptor labeled-particles had an acceptor concentration of 1 mol %. One sees in Figure 9 that when the interface is broad,

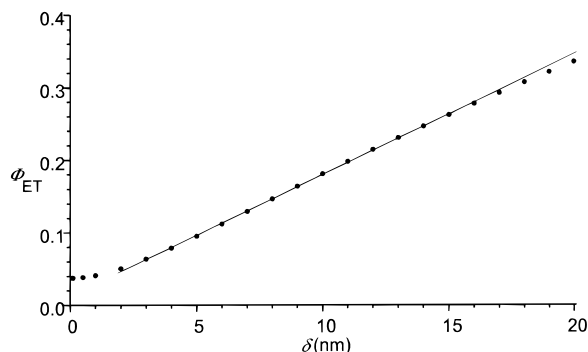


Figure 10. Energy transfer efficiency Φ_{ET} for simulated fluorescence decay curves with different interface thicknesses δ . Over the range of values of $\delta = 5$ –15 nm the efficiency of energy transfer is approximately proportional to the interface thickness. Below $\delta = 1$ nm the efficiency of energy transfer is approximately constant and equal to 4%.

there is a large rapid-decay contribution to the donor fluorescence at early times. For a broad interface, a large fraction of the donor and acceptor chromophores, bound to their respective polymers, are in proximity. As a consequence, the overall energy transfer rate increases.

From integration of the simulated fluorescence decay curves, we calculate the energy transfer quantum efficiency, eq II.2. In Figure 10 we plot Φ_{ET} calculated for the simulated fluorescence decay curves against the interface thickness. An approximately linear relation between Φ_{ET} and δ is obtained for interface thicknesses from $\delta = 5$ nm to $\delta = 15$ nm. The value of the energy transfer efficiency calculated for $\delta = 0$ nm represents the extent of energy transfer taking place across a perfectly sharp interface. For interfaces up to about $\delta = 1$ nm the efficiency of energy transfer is approximately constant and equal to 4%. There may be some differences in Φ_{ET} values computed here and those calculated from experimental decay profiles. The computed decay profiles were integrated numerically, whereas the experimental profiles were fitted first to a functional form¹ which is extrapolated to $t = \infty$ and then integrated analytically.

To obtain information about the interface thickness from the experimental fluorescence decay profiles, the experimental fluorescence decay profiles $I_D^{exp}(t)$ obtained for films of 1:1 blends of anthracene-labeled PEHMA and phenanthrene-labeled PEHMA-MAA latex particles were compared with simulated fluorescence decay profiles $I_D^{conv}(t)$. To evaluate the quality of the fitting results, we calculated the reduced χ^2 , the weighted residuals, and the autocorrelation of the residuals.

Two different blends of PEHMA and PEHMA-MAA are analyzed: one containing 11 mol % of MAA (D-MAA-11/PEHMA-A) and another containing 20 mol % of MAA (D-MAA-20/PEHMA-A). Experimental fluorescence decay profiles for films obtained from these blends were measured for different times of annealing at 60 °C and then fitted to the simulated decay profiles. In Figures 11 and 12 we show the reduced χ^2 obtained for these fits, plotted against the interface thickness, for films of D-MAA-11/PEHMA-A and D-MAA-20/PEHMA-A, respectively. Before annealing, the χ^2 profiles are very shallow for both samples, which means that the interface thickness can be defined with only limited precision. For D-MAA-11/PEHMA-A (Figure 11) the interface thickness is smaller than 4 nm, and for D-MAA-20/

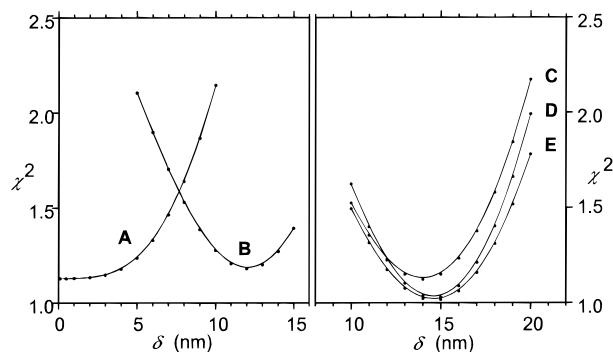


Figure 11. Reduced χ^2 plots from the fit of experimental fluorescence decay profiles obtained for films of 1:1 PEHMA and PEHMA-MAA blends containing 11 mol % of MAA, annealed at 60 °C for different times: no annealing (A); $t_{an} = 10$ min (B); $t_{an} = 30$ min (C); $t_{an} = 2$ h (D); and $t_{an} = 4$ h (E). Before annealing, the interface thickness is smaller than 4 nm, and after annealing it reaches an equilibrium value of $\delta = 15$ nm.

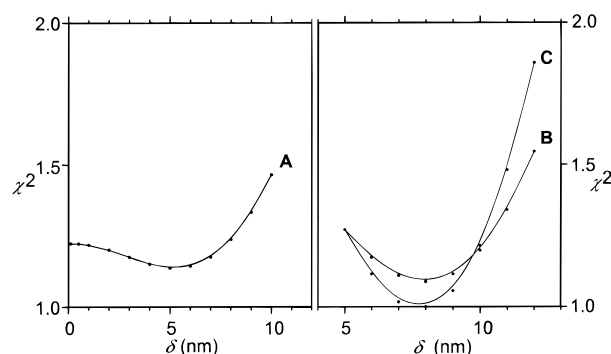


Figure 12. Reduced χ^2 plots from the fit of experimental fluorescence decay profiles obtained for films of 1:1 PEHMA and PEHMA-MAA blends containing 20 mol % of MAA, annealed at 60 °C for different times: no annealing (A); $t_{an} = 1$ h (B); and $t_{an} = 20$ h (C). Before annealing, the interface thickness is approximately equal to 5 nm, and after annealing it does not increase above $\delta = 8$ nm.

PEHMA-A (Figure 13) it is approximately equal to 5 nm. After annealing, the χ^2 profiles are sharper and the interface thickness is well-defined. For D-MAA-11/PEHMA-A we obtain a best-fit equilibrium value of $\delta = 15$ nm, whereas for D-MAA-20/PEHMA-A, the interface thickness does not increase above $\delta = 8$ nm. These results confirm that polymer containing 20 mol % MAA is less miscible with PEHMA than the polymer containing 11 mol % MAA.

From the plots of the reduced χ^2 shown in Figures 11 and 12, we can detect differences in the precision with which we can calculate the value of interface thickness δ . The χ^2 profile is shallow for the samples with no annealing and sharper after the same samples are annealed. It is however difficult to decide precisely from these plots which δ values are acceptable for each decay profile. A better way to determine the optimum fit for the experimental decay profiles and the error bars for the interface thickness values is by inspection of the autocorrelation plots. The fitting results for the experimental fluorescence decay profiles of dispersion-cast films containing latex with 11 mol % of MAA are shown in Figure 13. For the decay measured before the film was annealed (Figure 13a), we obtain acceptable autocorrelations of the weighted residuals for all interface widths from $\delta = 0$ nm to $\delta = 4$ nm. For $\delta = 5$ nm significant deviations are observed, indicating that the

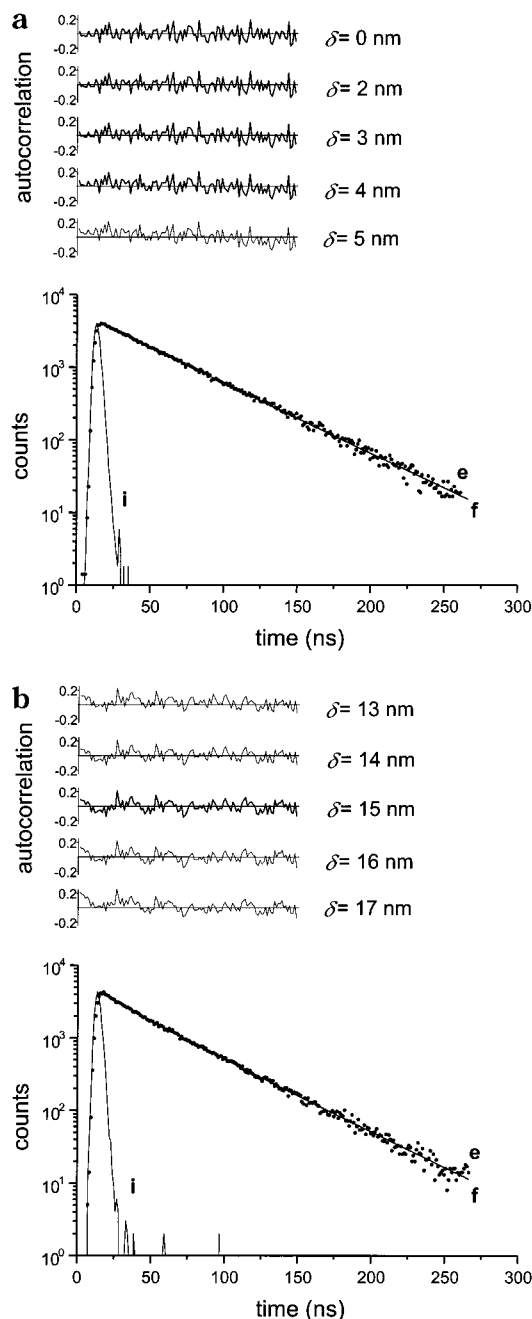


Figure 13. Experimental instrument response function (i) and experimental donor decay profile of a film of 1:1 blend of PEHMA and PEHMA-MAA, containing 11 mol % of MAA. (a) Before annealing (e), fitted to a decay simulated with $\delta = 3$ nm (f). The autocorrelation functions relative to the fitting of the curves simulated with interface thickness of $\delta = 0$ –4 nm are well distributed, but even for $\delta = 5$ nm some deviation is observed. (b) After 4 h of annealing (e) and fitted to a decay simulated with $\delta = 15$ nm (f). The autocorrelation functions relative to the fitting of the curves simulated with interface thickness of $\delta = 14$ –16 nm are well distributed. For $\delta = 13$ and 17 nm some deviation is observed in the autocorrelation function.

decay profile simulated for this thickness does not fit the experimental decay. In this way we can define the interface width and respective error bar for the unannealed film as $\delta = 2 \pm 2$ nm. After annealing this film for 4 h, the fluorescence decay is faster and is best fitted by the curve simulated for an interface width of $\delta = 15$ nm (Figure 13b), with the autocorrelation of the residuals for the fittings with $\delta = 14$ nm and $\delta = 16$ nm also

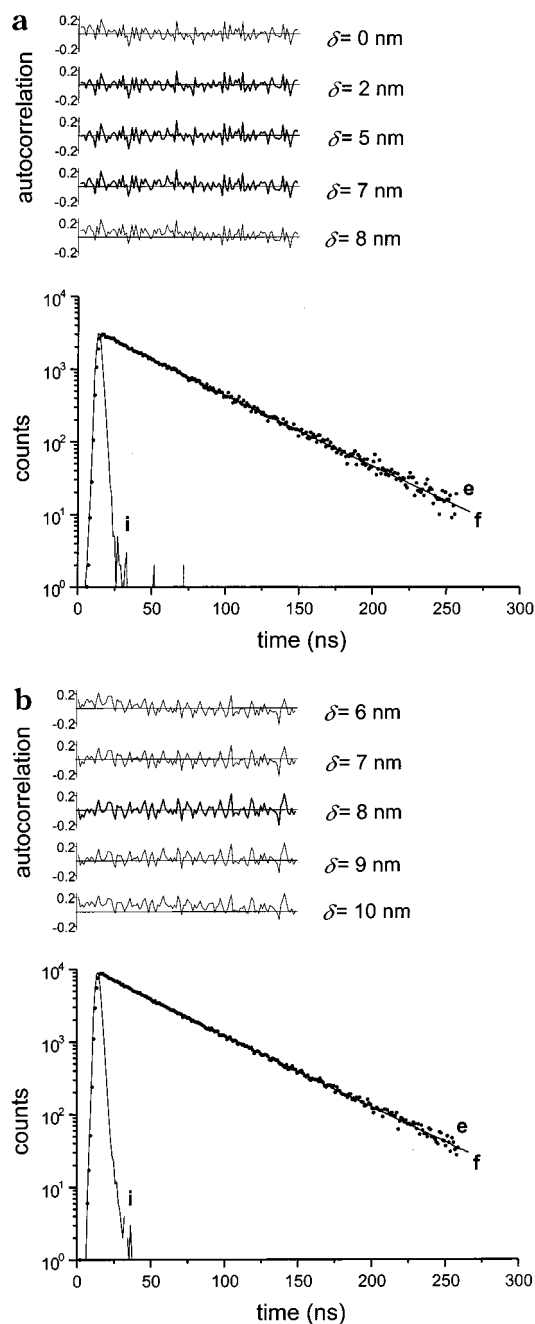


Figure 14. Experimental instrument response function (i) and experimental donor decay profile of a film of 1:1 blend of PEHMA and PEHMA-MAA containing 20 mol % of MAA. (a) Before annealing (e) and fitted to a decay simulated with $\delta = 5$ nm (f). The autocorrelation functions relative to the fitting of the curves simulated with interface thickness of $\delta = 2$ –7 nm are well distributed. For $\delta = 0$ and 8 nm some deviation is observed in the autocorrelation function. (b) After 20 h of annealing (e) and fitted to a decay simulated with $\delta = 8$ nm (f). The autocorrelation functions relative to the fitting of the curves simulated with interface thickness of $\delta = 7$ –9 nm are well distributed. For $\delta = 6$ and 10 nm some deviation is observed in the autocorrelation function.

acceptable.

The experimental fluorescence decay profiles of films containing latex with 20 mol % of MAA (Figure 14) show less energy transfer than the corresponding decays obtained for film with 10 mol % of MAA. The decay curve obtained before the film was annealed (Figure 14a) can be well fitted by all curves simulated for interface thicknesses ranging from $\delta = 2$ nm to $\delta = 7$

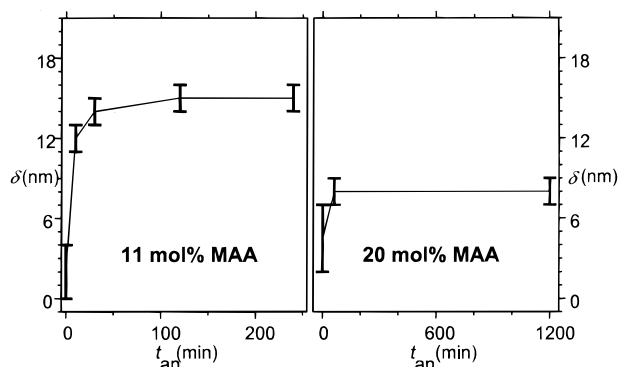


Figure 15. Evolution of the interface thickness δ with annealing time t_{an} for 1:1 blends of PEHMA and PEHMA-MAA containing 10 and 20 mol % of MAA. Error bars were obtained using the procedure described in Figures 14 and 15.

nm. After annealing the sample for 20 h, the fluorescence decay is slightly faster and can be fitted by the curves simulated for interface thicknesses of $\delta = 7$ nm and $\delta = 9$ nm, with $\delta = 8$ nm giving the best fit (Figure 14b).

Using the procedure described above, we define the values of the best-fit interface thickness for each decay and the respective error bars. The evolution of the obtained interface thickness with annealing time is shown in Figure 15 for the samples containing latex with 11 and 20 mol % of MAA. For long annealing times, the systems converge to an equilibrium state with thick interfaces.

Estimating the Flory–Huggins χ Parameter. In the preceding paper,¹ we considered the relationship between the interface thickness δ and the Flory–Huggins χ parameter. The appropriate expression (eq 15, preceding paper) has two terms: one which depends on δ and one which accommodates the effect of finite polymer chain length.²¹ We use this approach to calculate a value of $\chi \approx 0.036$ for the blend of D-MAA-11 + PEHMA-A and a value of $\chi \approx 0.05$ for the blend of D-MAA-20 + PEHMA-A. These numbers are reasonable in magnitude but should be treated as rough estimates.

It is not hard to identify the origin of the limited miscibility of PEHMA with its carboxyl-containing copolymer. In nonpolar media, $-\text{COOH}$ groups form a planar dimer held together by a pair of hydrogen bonds, and at higher concentrations, aggregation of the $-\text{COOH}$ groups can occur. Diluting the P(EHMA-*co*-MAA) polymer with PEHMA itself must either decrease the number of hydrogen bonds in the system or decrease the entropy of association. Either of these effects would provide a driving force for phase separation.

Conclusions

Polymer Miscibility. We examined the miscibility of blends of PEHMA latex copolymers using the DET technique. When films were formed by mixing Phe- and An-labeled PHEMA homopolymer latex dispersions and drying the dispersion at 4 °C, very little ET was observed ($\Phi_{ET} = 0.06$). This value of Φ_{ET} is consistent with ET from excited donors near the edge of one cell in the film transferring energy to acceptors across the boundary in an adjacent cell. When these films were annealed at 60 °C, we observed an increase in ET, which leveled off at $\Phi_{ET} = 0.52$. Upon annealing of latex films for long times, polymer diffusion leads to complete mixing of the polymers originally confined to separated

cells in the film. From an ET perspective, full mixing corresponds to films in which the donors and acceptors are randomly distributed. In this case, the magnitude of Φ_{ET} depends on R_0 and the (uniform) concentration of acceptor groups in the film. We expect and find that the magnitude of Φ_{ET} obtained from solvent-cast films is the same as that obtained from latex films annealed for long times. From the perspective of polymer diffusion in latex films, full mixing corresponds to polymer diffusion over a length scale comparable to a particle radius.

We were careful to prepare all samples in the form of particles of similar size, with essentially identical label content. As a consequence, we find that random mixing of any pair of donor- and acceptor-labeled polymer described here yields $\Phi_{ET} = 0.52$. Thus, values of $\Phi_{ET} < 0.52$ for solvent-cast films or latex films annealed for long times are a signature of phase separation in the system. For example, when 11 mol % of MAA is incorporated in one of the two latex polymers, the miscibility is reduced significantly ($\Phi_{ET} = 0.24$) and reduced further when the amount of MAA is doubled ($\Phi_{ET} = 0.16$).²² Solvent-cast films of these polymer blends exhibit Φ_{ET} values on the order of 0.4, indicating that some phase segregation occurs upon solvent evaporation. Upon annealing, further demixing occurs, and the system evolves to the same value of Φ_{ET} as found in the latex film.

While one expects identical values of Φ_{ET} for solvent-cast films and annealed latex films for miscible polymer mixtures, there is no reason to expect this behavior for blends of limited miscibility. For these types of blends, the extent of mixing is determined by the product of the interface thickness and the interfacial area between the two types of polymers. For example, Feng et al.²³ have shown that, in blends of PMMA nanospheres with PEHMA with a constant volume fraction of PMMA, the extent of ET is larger for blends prepared from smaller diameter PMMA particles. The Φ_{ET} values increase in proportion to the surface-to-volume ratio in the mixtures. In this context, it may be a coincidence that we obtain identical Φ_{ET} values for the annealed solvent-cast blends and latex blends of PEHMA with P(EHMA-*co*-MAA).

Some of the most interesting results obtained in these studies concern the reactive blends of D-MAA-11 plus A-tBCEMA-11 and D-MAA-20 plus A-tBCEMA-11. Φ_{ET} values of solvent-cast films prepared from freeze-dried mixtures of the two polymers show significant demixing (Figures 5–7). Yet when the films were annealed, Φ_{ET} values evolved to that (0.52) consistent with full miscibility of the two components. Miscibility must be driven by the reaction of the $-\text{N}=\text{C}=\text{N}-$ groups in one polymer with the $-\text{COOH}$ groups in the other polymer. FTIR studies (Figure 7) demonstrate that miscibility in the solvent-cast films increases in parallel with consumption of the carbodiimide groups. Model experiments suggest that the increased miscibility arises partially from the higher compatibility of $-\text{COOH}$ and dialkyl urea groups, but also from graft copolymer formation.

Polymer Interfaces. In the preceding paper,¹ we presented a model for describing the shape of fluorescence decay profiles in systems characterized by ET from donor-labeled spheres to acceptor-labeled surroundings. The model assumes a Helfand–Tagami distribution of polymer segments across the interface.

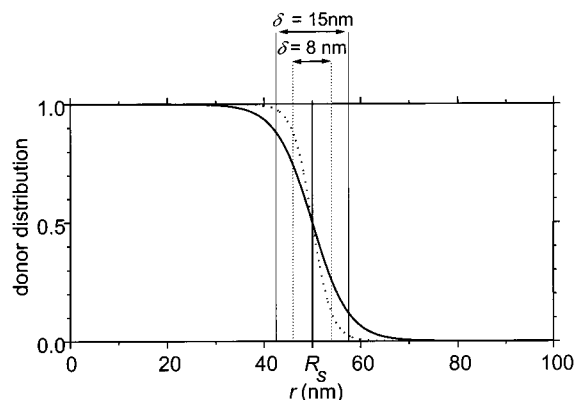


Figure 16. Donor distribution functions calculated for particles with radius $R_s = 50$ nm and an interface thickness obtained after annealing 1:1 blends of PEHMA and PEHMA-MAA. For the polymer containing 11 mol % of MAA the interface thickness is $\delta = 15$ nm, while for the sample with 20 mol % of MAA the interface thickness is $\delta = 8$ nm.

Data analysis involves comparing experimental decay profiles with those obtained by simulations. When we apply this model to the characterization of the latex blends PEHMA-P(EHMA-co-MAA) described above, we are able to infer values of the interface thickness.

For latex films of D-MAA-11 plus A-PEHMA prepared at 4 °C, where $\Phi_{ET} = 0.06$, the interface is thin. Any value of δ between 0 and 4 nm is consistent with the experiments. As the sample is annealed, the interface evolves and eventually reaches 15 nm. Similar behavior is found for the latex blend of D-MAA-20 plus A-PEHMA. Here the limiting interface thickness is 8 nm. We summarize our description of the two polymer blends at equilibrium in Figure 16. Here we plot the polymer segment density distribution across the polymer interface for pairs of polymers with the properties of the blend of MAA-11 with PEHMA (solid line) and the blend of MAA-20 with PEHMA (dotted line). The former is characterized by $\delta = 15$ nm. The dotted line corresponds to a blend with $\delta = 8$ nm.

In Figure 10, we plot values of Φ_{ET} using the results of our simulations. We can use this plot to estimate values of δ from measured values of Φ_{ET} . Taking Φ_{ET} values from Figure 4 (D-MAA-20 plus A-PEHMA), we estimate that the latex film prepared at 4 °C has an interface thickness as large as 3 nm. After a few minutes of annealing, when $\Phi_{ET} = 0.10$, $\delta \approx 5.2$ nm. When $\Phi_{ET} = 0.13$, $\delta \approx 6.6$ nm. The limiting value of Φ_{ET} corresponds to $\delta \approx 9$ nm. Taking Φ_{ET} values from Figure 3 (D-MAA-11 plus A-PEHMA), we estimate that the latex film prepared at 4 °C has an interface thickness on the order of 3 nm. After a few minutes of annealing, when $\Phi_{ET} = 0.21$, $\delta \approx 12$ nm. The limiting value $\Phi_{ET} = 0.24$ corresponds to $\delta \approx 13$ nm. From this exercise, we learn that values of the interface thickness deduced from experimental values of Φ_{ET} are similar to those inferred by direct examination of the donor fluorescence decay profiles. We see that values of the interface thickness inferred from experimental values of Φ_{ET} are similar to those obtainable by more elaborate analyses of the donor fluorescence decay profiles. One has to make sure, however, that the parameters R_s , R_0 , τ_D , R_e , and k^2 of the simulations used to obtain the master curve are appropriate to the system examined experimentally.

One may ask why we do not extend this analysis to the other latex blend systems in which we plot Φ_{ET} against annealing time. Here we must remember that

the simulations assume a Helfand-Tagami polymer segment density profile across the interface. This profile is appropriate for blends of limited miscibility, but it is not appropriate to other processes such as diffusion across an interface between two miscible polymers. For low molecular weight polymers, this type of diffusion leads to a Fickian segment density profile. For entangled polymers, diffusion across an interface generates a different segment density profile.²⁴ To calculate interdiffusion distances from the $I_D(t)$ decay curves, one has to compare the measured decay profiles with simulated data that take proper account of the underlying physics.^{25,26} This is a very important task for reactive blends such as P(EHMA-co-MAA) + P(EHMA-co-tBCEMA). Here, however, we lack a fundamental theory describing the nature of polymer diffusion across interfaces when diffusion is coupled to a chemical reaction that retards or stops the diffusion of the molecules that have reacted.

Acknowledgment. We thank ESTAC Canada and NSERC Canada for their financial support. J. P. S. Farinha acknowledges the support of FCT-PRAXIS XXI.

References and Notes

- (1) Farinha, J. P. S.; Vorobyova, O.; Winnik, M. A. *Macromolecules* **2000**, *33*, 5863.
- (2) Helfand, E.; Tagami, Y. *J. Chem. Phys.* **1972**, *56*, 3592.
- (3) Klafter, J.; Blumen, A.; Zumhofen, G. *J. Chem. Phys.* **1986**, *84*, 1397.
- (4) (a) Morawetz, H. *Science* **1979**, *203*, 405. (b) Morawetz, H. *Science* **1988**, *240*, 172. (c) Morawetz, H. *J. Polym. Sci., Part A: Polym. Chem.* **1999**, *37*, 1725.
- (5) (a) Winnik, M. A. *Curr. Opin. Colloid Interface Sci.* **1997**, *2*, 192. (b) Winnik, M. A. In *Emulsion Polymerization and Emulsion Polymers*; Lovell, P. A., El-Aasser, M. S., Eds.; Wiley: New York, 1997; p 458. (c) Keddie, J. L. *Mater. Sci. Eng.* **1997**, *21*, 101.
- (6) Taylor, J. W.; Bassett, D. R. *ACS Symp. Ser.* **1997**, *663*, 137.
- (7) Feng, J.; Winnik, M. A. *Macromolecules* **1997**, *30*, 4324.
- (8) Dolphin, D.; Wick, A. *Tabulation of Infrared Spectral Data*; Wiley-Interscience: New York, 1977.
- (9) Kim, H.-B.; Wang, Y.; Winnik, M. A. *Polymer* **1994**, *35*, 1779.
- (10) (a) Zhao, C. L.; Wang, Y.; Hruska, Z.; Winnik, M. A. *Macromolecules* **1990**, *23*, 4082. (b) Winnik, M. A.; Wang, Y.; Haley, F. J. *Coat. Technol.* **1992**, *64* (811), 51. (c) Juhue, D.; Wang, Y.; Winnik, M. A. *Makromol. Chem., Rapid Commun.* **1993**, *14*, 345. (d) Winnik, M. A.; Li, L.; Liu, Y. S. In *Microchemistry: Spectroscopy and Chemistry in Small Domains*; Masuhara, H., Kitamura, N., Eds.; Elsevier: Amsterdam, 1994; p 387. (e) Liu, Y. S.; Feng, J.; Li, L.; Winnik, M. A. *J. Chem. Phys.* **1994**, *101*, 9096.
- (11) Feng, J. Ph.D. Thesis, University of Toronto, 1998.
- (12) Pham, H. H.; Winnik, M. A. *J. Polym. Sci., Part A: Polym. Chem.* **2000**, *38*, 855.
- (13) Pham, H. H. Ph.D. Thesis, University of Toronto, 2000.
- (14) Xu, Z.; Lu, G.; Cheng, S.; Li, L. *J. Appl. Polym. Sci.* **1995**, *56*, 575.
- (15) Versteegen, J. M. G. Ph.D. Thesis, University of Eindhoven, 1998.
- (16) O'Connor, D.; Phillips, D. *Time-Resolved Single-Photon Counting*; Academic Press: New York, 1984.
- (17) Wang, Y.; Zhao, C. L.; Winnik, M. A. *J. Chem. Phys.* **1991**, *95*, 2143.
- (18) Brandrup, J.; Immergut, E. H., Eds. *Polymer Handbook*, 3rd ed.; John Wiley & Sons: New York, 1989.
- (19) Doi, M.; Edwards, S. *The Theory of Polymer Dynamics*; Oxford Press: New York, 1986.
- (20) Yekta, A.; Winnik, M. A.; Farinha, J. P. S.; Martinho, J. M. G. *J. Phys. Chem. A* **1997**, *101*, 1787.
- (21) Stamm, M.; Schubert, D. W. *Annu. Rev. Mater. Sci.* **1995**, *25*, 325.
- (22) Some further insights are available from our estimates of the Flory-Huggins χ parameter for these two blends: $\chi \approx 0.036$

- for (D-MAA-11 + PEHMA-A) and $\chi \approx 0.05$ for (D-MAA-20 + PEHMA-A). Using these values and the number-averaged degree of polymerization (N) of the components, we estimate $\chi(N_{\text{PEHMA}} + N_{\text{MAA-11}})$ to be 14 and $\chi(N_{\text{PEHMA}} + N_{\text{MAA-20}})$ to be 20.
- (23) Feng, J.; Yekta, A.; Winnik, M. A. *Chem. Phys. Lett.* **1996**, 260, 296.
- (24) (a) de Gennes, P. G. *C. R. Acad. Sci. (Paris)* **1980**, 291, 219.
(b) Prager, S.; Tirrell, M. *J. Chem. Phys.* **1981**, 75, 5194. (c) Wool, R. P.; O'Connor, K. M. *J. Appl. Phys.* **1981**, 52, 5953.
(d) Kim, Y.-H.; Wool, R. P.; O'Connor, K. M. *Macromolecules* **1983**, 16, 1115.
- (25) Farinha, J. P. S.; Martinho, J. M. G.; Yekta, A.; Winnik, M. A. *Macromolecules* **1995**, 28, 6084.
- (26) Farinha, J. P. S.; Martinho, J. M. G.; Kawaguchi, S.; Yekta, A.; Winnik, M. A. *J. Phys. Chem.* **1996**, 100, 12552.

MA991832O